2015 5th Australian Control Conference (AUCC)
November 5-6, 2015. Gold Coast, Australia

Steady-state and transient dynamic behavior of simple climate models for application in integrated assessment models

Salman Hafeez, Steven R. Weller, and Christopher M. Kellett

Abstract— **We characterize the steady-state and transient dynamic behavior of a suite of twelve linear time-invariant (LTI) climate models capturing the response of global mean surface temperature to net radiative forcing. The LTI models considered here have previously been obtained by system identification experiments with data derived from the Coupled Model Intercomparison Project phase 3 (CMIP3), and have subsequently been applied in integrated assessment models (IAMs) of climate–economy based on the solution of a finite-horizon nonlinear optimal control problem, where atmosphere–ocean general circulation models (AOGCMs) of the climate are computationally prohibitive. In this paper, we compute the equilibrium climate sensitivity (ECS) and transient climate response (TCR) for each of the twelve LTI climate models in the model suite, and compare the values so obtained with previously published values of ECS and TCR for these CMIP3 models. The results of this paper confirm the suitability of simple LTI climate models in IAMs, and validate the robustness of conclusions drawn from the application of such models in integrated climate–economy assessments.**

I. INTRODUCTION

Anthropogenic climate change, principally arising from the accumulation of atmospheric greenhouse gases (GHGs) as a consequence of fossil fuel combustion, poses significant physical, social, and economic risks. To quantify both the economic costs and scientific uncertainties associated with the build-up of GHGs such as carbon dioxide (CO_2) in the atmosphere, economists employ integrated assessment models (IAMs) which couple simplified models of the global system in feedback connection with stylized representations of global macroeconomic behavior.

Comprehensive climate representations in the form of atmosphere–ocean general circulation models (AOGCMs) simulate the climatic response of the atmosphere, ocean, land, and cryosphere to the planetary top-of-atmosphere energy imbalance between absorbed sunlight (short wave radiation) and emitted thermal (longwave) radiation, the so-called *radiative forcing*. AOGCMs are fundamentally ill-suited to direct application in IAMs, however, on account of their computational intensity. For example, the CSIRO Mk3L model takes on the order of 6 weeks on a typical desktop PC to simulate 1000 years of climatic response [1].

One approach is to use so-called reduced-complexity climate models, of which MAGICC (Model for the Assessment of Greenhouse-gas Induced Climate Change) is by far the most widely-used example [2]. Nevertheless, the MAGICC model itself is nonlinear, high-order ($\approx$100 states), and time-varying, thereby limiting the direct applicability of MAGICC for IAMs based on numerical optimization. A prominent application of IAMs is the estimation of the social cost of carbon (SCC), defined as the net present value of an incremental increase in CO_2 emissions, expressed as a dollar cost per metric ton of CO_2. Estimating the SCC using the widely-used DICE (Dynamic Integrated model of Climate and the Economy) IAM, for example, requires the solution of a finite-horizon nonlinear optimal control problem [3], [4], [5]. In such a setting, the structure of the climate model has a major influence on the feasibility of computing an optimal solution; consequently even reduced-complexity climate models such as MAGICC are far too complex for direct application in IAM-based computation of the SCC.

Given these computational considerations, simple climate models are preferred in the most widely-used IAMs such as DICE [3], FUND [6] and PAGE [7]. For example, in the DICE IAM used by the U.S. government's Interagency Working Group (IAWG) on Social Cost of Carbon [8], [9], the climatic response to forcing is modeled using a second-order, single-input single-output (SISO), linear time-invariant (SISO) system. The input to the DICE-2013R climate model is the average planetary radiative forcing, and the output is global mean surface temperature measured as an anomaly relative to the baseline year 1900 [3], [10]. Here and elsewhere, temperature anomalies serve as a simple, if imperfect, proxy for broader climatic change, e.g. patterns and amounts of precipitation, reduced ice and snow cover, and increasing sea levels.

System identification techniques were used in [11] to obtain low-order ($n = 4$) LTI approximations to 12 AOGCMs appearing in the Coupled Model Intercomparison Project phase 3 (CMIP3) multimodel ensemble, and for which MAGICC6 emulations are available [2]. This collection of 12 LTI models was subsequently used in the estimation of the SCC [4], with the cost of CO_2 emissions in 2010 estimated to lie in the range US\$8.50–US\$49.00 per ton of CO_2, depending on the CMIP3 climate model employed. While the wide variability in the range of SCC estimates serves to highlight the economic ramifications of scientific uncertainty in the climatic response to radiative forcing caused by anthropogenic CO_2 emissions, it is imperative to ensure that the approximation of highly complex AOGCMs with simple LTI representations faithfully captures key properties of the dynamic response of each of the more complex models.

In the climate science literature, two scalar parameters

Salman Hafeez, Steven R. Weller, and Christopher M. Kellett are with the School of Electrical Engineering and Computer Science, University of Newcastle, Callaghan, NSW 2308, Australia salman.hafeez@uon.edu.au, {steven.weller,chris.kellett}@newcastle.edu.au

C. M. Kellett is supported by ARC Future Fellowship FT1101000746

find widespread application in characterizing the climate response to radiative forcing. Specifically, the *equilibrium climate sensitivity (ECS)* and *transient climate response (TCR)*, which succinctly quantify the magnitude and speed of the temperature response to forcing, respectively. Formal definitions of ECS and TCR are given in Section II.

In this paper, we compute the ECS and TCR for each of the 12 low-order LTI climate models presented in [11], and compare the results with published values obtained directly from the AOGCMs [12]. We further confirm that each of the 12 models considered is characterized by a decomposition into clearly separated fast and slow components, consistent with the known thermal capacities of the upper (mixed) layer and deep ocean, respectively. Finally, we confirm minimal loss in precision in down-sampling the 1-year sampled models from [11] for use in the 5-year sampled DICE-2013R IAM [3], [10]. These results confirm the suitability of simple LTI climate models [11] in IAMs, and validate the robustness of conclusions drawn from the application of such models in integrated climate–economy assessments based on the solution of nonlinear optimal control problems [4].

The paper is organized as follows. Background on IAMs, the CMIP3 ensemble, and ECS/TCR are given in Section II. Experimental methods and results are presented in Section III. Brief conclusions are drawn in Section IV.

II. BACKGROUND

A. Integrated Assessment Models (IAMs)

The motivating context for the simple climate models considered in this paper are IAMs for climate–economy assessments. In such models, geophysical and economic sub-models are considered to be in feedback connection as shown in Fig. 1. Anthropogenic CO_2 emissions E (GtC yr^{-1}, 1 GtC $= 10^{15}$ g C) arising from economic activity result in elevated atmospheric carbon stocks M (GtC) which give rise to net positive radiative forcing F (W/m^2) at the top of atmosphere via the enhanced greenhouse effect, with F depending logarithmically on anomalous atmospheric CO_2 [2]. Consequently, warming of the Earth system—here measured by the increase in global mean surface temperature $T(°C)$—impacts on gross domestic product via a temperature-dependent damage function within the "economy" block in Fig. 1.

IAMs are a common tool in environmental economics for devising and assessing strategies to address the risks of anthropogenic climate change. Using the high-level structure shown in Fig. 1, for example, the DICE IAM can be used to compute an economically optimal CO_2 emissions trajectory, in which a discounted sum of the utility of economic consumption C is maximized by means of an optimized schedule of CO_2 emissions reduction rates μ and the fraction s of the global economic output which is saved; see [3], [4], [10] for details. Computing the optimal emissions trajectory requires the solution of an optimal control problem, and yields the economically optimal price on CO_2 emissions as a by-product [3], [8].

The feedback interconnection of the geophysical and economic sub-blocks, intrinsic to IAMs, together with the central role played by optimal control problems in economic decision-making, underscores the relevance of IAMs to the systems and control community.

In this paper, the climate models of interest capture the dynamic response of global mean surface temperature anomalies T to net radiative forcing F, as shown in Fig. 1. In particular, we are interested in quantifying both the steady-state and transient behavior of such climate models—essentially their DC gain and speed of response, in a sense to be made precise in Section II-C below, using terminology drawn from the climate science literature.

The closed-loop response of the IAM in Fig. 1 necessarily depends on the dynamics of the carbon cycle, the global economy and the static (logarithmic) nonlinear dependence of radiative forcing on atmospheric carbon load measured relative to pre-industrial times, c. 1750. Nevertheless, at least insofar as the geophysical sub-model in Fig. 1 is concerned, it is scientific uncertainty regarding both the strength and speed of the climatic response to radiative forcing which overwhelmingly influences the feasibility of 2 °C warming relative to pre-industrial levels, a level widely recognized as a key threshold for dangerous climate change [13].

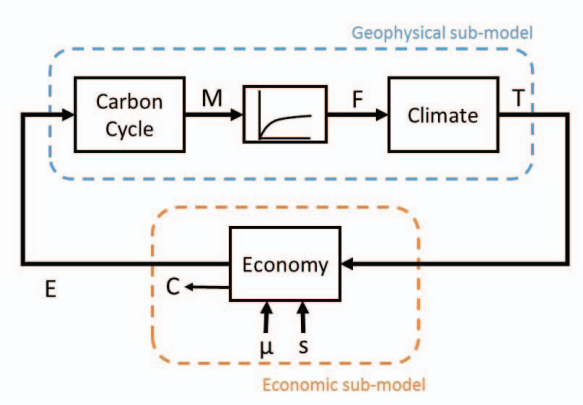

Fig. 1. High-level representation of an IAM: M is the mass of carbon in the atmosphere, F is the net radiative forcing, T is the global mean surface atmospheric temperature anomaly relative to the year-1900 mean, C is global economic consumption (2005 $US trillions per year), μ is the emission control rate, and s is the share of net economic output which is invested in productive capital

B. Climate models and the CMIP3 ensemble

This paper employs a set of 12 climate models derived from a multimodel dataset known as the Coupled Model Intercomparison Project phase 3 (CMIP3), a project of the World Climate Research Programme. The CMIP3 dataset is a compilation of AOGCM simulation data submitted from 14 modeling groups for a total of 23 AOGCMs in preparation for the Fourth Assessment Report (AR4) of the Intergovernmental Panel on Climate Change (IPCC) [12], [14], [15]. The CMIP3 ensemble therefore represents a broad range of plausible climatic responses to radiative forcing.

Derivation of the 12 climate models in [11] is indirect, and uses the emulation of CMIP3 AOGCMs via the MAGICC reduced-complexity climate model as an intermediate step. A

key motivation for the present paper, therefore, is to quantify the accuracy with which the indirect derivation of the climate models in [11] retains the crucial steady-state and transient dynamic response characteristics of each of the underlying CMIP3 climate models [16]. The discrete-time models in [11] employ a 1-year sample period, whereas the climate models in the "vanilla" DICE-2013R IAM use a 5-year sample period [3], [10]. It is therefore also of interest to quantify the extent to which down-sampling of the models in [11] to a 5-year sample period results in loss of model integrity for the purposes of integrated assessment modeling.

C. ECS and TCR

Since the pioneering research of Arrhenius in the late 19-th century, scientists have sought to quantify the warming impact of increased atmospheric CO_2 due to the enhanced greenhouse effect. By far the most widely used metric for such quantification is the *equilibrium climate sensitivity (ECS)*, defined as the long-term increase in global mean surface temperature under an assumed doubling of atmospheric CO_2 concentrations.

Exploiting the well-known (logarithmic) relation between CO_2 concentration and forcing [2] enables the ECS to be equivalently considered as the steady-state increase in global mean surface temperature in response to a 3.8 W/m^2 increase in net radiative forcing [10]. In the most recent Fifth Assessment Report (AR5) of the IPCC, the ECS is deemed as being "likely in the range 1.5 °C to 4.5 °C, extremely unlikely less than 1 °C, and very unlikely greater than 6 °C" [17, p.16].

While the strength of the steady-state response to forcing, as captured by the ECS, is clearly a basic property of the climate system, so too is the speed of response. This is especially true in the integrated assessment setting, where the policy-relevance of the long-term response is not immediately clear given the centennial timescales of the thermal response of the deep ocean to radiative forcing.

In the IAM literature, therefore, it is commonplace to quantify the speed of response via the *transient climate response (TCR)*, defined as the globally averaged surface air temperature change at the time of CO_2 doubling assuming annual 1% increases in CO_2 concentration. Given the logarithmic dependence of forcing on CO_2 concentrations, the TCR can be calculated as the temperature at 70 years in response to a linear ramp increase in forcing from 0 to 3.8 W/m^2 over 70 years, and held constant thereafter [16]; the significance of "70" here arising from $1.01^{70} = 2.00$, i.e. compounded annual 1% increases leading to a doubling after 70 years.

III. METHODS AND RESULTS

To estimate the ECS and TCR for each of the 12 CMIP3 models in [11], we simulate the response of each model to a linear ramp increase in radiative forcing, rising from 0 to 3.8 W/m^2 over a 70-year period, as described in Section II-C. The TCR is then estimated as the temperature output of the climate model at 70 years, while the ECS is taken as the output at 1000 years, by which time the transient response is deemed to have effectively disappeared; see Fig. 2. The results of these experiments are reported in Table I and Figs. 3 and 4, labeled in each case via the sample period $\Delta = 1$ year.

TABLE I

EQUILIBRIUM CLIMATE SENSITIVITY (ECS) AND TRANSIENT CLIMATE RESPONSE (TCR) FOR LTI APPROX. OF CMIP3 MODELS, AND VALUES REPORTED IN IPCC AR4. SAMPLE PERIODS $\Delta = 1$ AND $\Delta = 5$ YEARS

Model	Estimated				IPCC AR4	
	ECS		TCR		ECS	TCR
	$\Delta = 1$	$\Delta = 5$	$\Delta = 1$	$\Delta = 5$	$\Delta = 1$	$\Delta = 1$
CGCM3.1(T47)	3.21	3.21	2.32	2.26	3.4	1.9
CNRM-CM3	3.01	3.01	2.11	2.06	N.A.	1.6
CSIRO-Mk3.0	2.23	2.24	1.47	1.43	3.1	1.4
ECHO-G	2.60	2.60	2.08	2.01	3.2	1.7
GISS-EH	2.16	2.16	1.58	1.55	2.7	1.6
INM-CM3.0	2.30	2.30	1.81	1.76	2.1	1.6
IPSL-CM4	4.00	4.02	2.43	2.36	4.4	2.1
MIROC3.2(H)	5.94	5.95	3.32	3.2	4.3	2.6
MIROC3.2(M)	4.16	4.18	2.36	2.28	4.0	2.1
MRI-CGCM2.3.2	2.54	2.54	1.88	1.83	3.2	2.2
PCM	1.86	1.86	1.47	1.44	2.1	1.3
UKMO-HadCM3	3.01	3.01	2.15	2.08	3.3	2.0

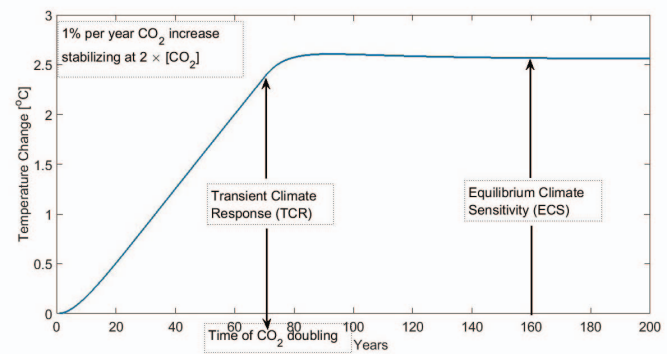

Fig. 2. Global mean temperature change for 1%/yr increase in CO_2 concentration, with subsequent stabilization at $2\times CO_2$. The TCR is the temperature increase at the time of atmospheric CO_2 concentration doubling, and the ECS is the temperature change after the system has reached a new thermal equilibrium with doubled CO_2.

Also shown in Table I and Figs. 3 and 4 are the ECS and TCR values obtained from down-sampled CMIP3-derived models, denoted by sample period $\Delta = 5$ years as per the requirements of the vanilla DICE-2013R IAM, and the ECS/TCR values of the full-complexity CMIP3 models [16], denoted as "IPCC". Downsampling is performed by first computing an underlying continuous-time model under zero-order hold (ZOH)-equivalence via MATLAB's `d2c` command, then re-sampling with a $\Delta = 5$ year period using `c2d`.

In the Appendix are presented the coefficients of each of the 12 CMIP3-derived models, downsampled with period $\Delta = 5$ years as required by the DICE-2013R IAM. The coefficient data in the Appendix follows the format shown

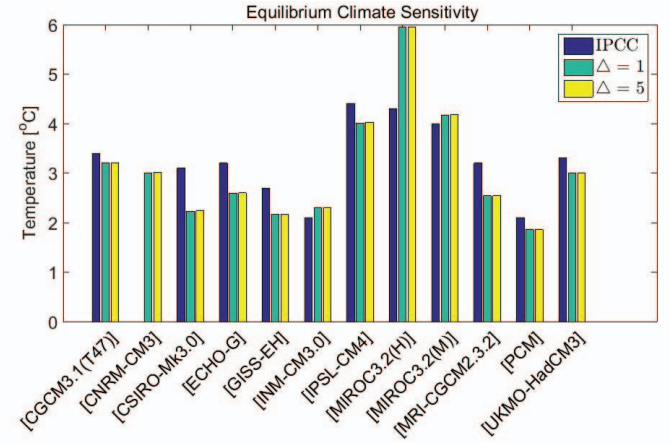

Fig. 3. ECS for 12 full-complexity CMIP3 models reported in AR4 ("IPCC"), and their corresponding values for LTI approximations with sample period $\Delta = 1$-year from [11] and down-sampled to $\Delta = 5$-years

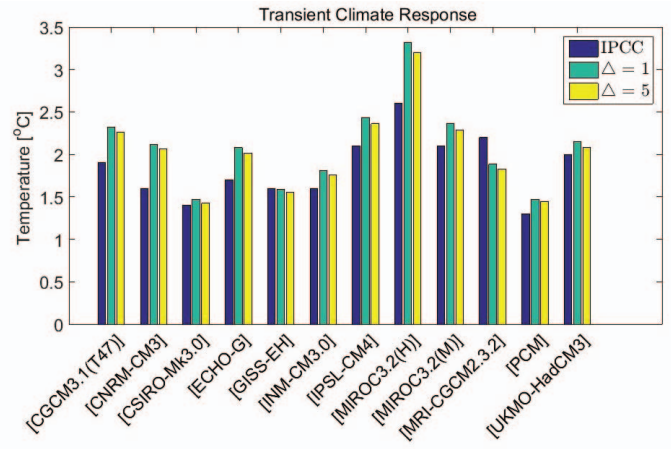

Fig. 4. TCR for 12 full-complexity CMIP3 models reported in AR4 ("IPCC"), and their corresponding values for LTI approximations with sample period $\Delta = 1$-year from [11] and down-sampled to $\Delta = 5$-years

in Table II, where the climate models take the form

$$G(q) = \frac{b_0 + b_1 q^{-1} + \cdots + b_4 q^{-4}}{1 + a_1 q^{-1} + \cdots + a_4 q^{-4}},$$

where q is the forward shift operator.

For both ECS and TCR, there is negligible difference between the values reported for $\Delta = 1$ and $\Delta = 5$, confirming that the downsampling of the annually-sampled models in [11] for application in DICE-2013R [4] results in only a very minor loss of precision.

For most of the 12 CMIP3 models considered, the correspondence between the underlying "true" values of ECS and TCR [16], and the order $n = 4$ LTI approximations is of the order of $\sim 10\%$ for ECS, and $\sim 20\%$ for TCR. Moreover for most models, the true ECS is under-estimated by the low-order approximations, whereas for TCR it is over-estimated.

Given the substantial reduction in computational complexity between the underlying AOGCMs and their low-order LTI approximations, the suitability (or otherwise) of the simple models would depend on the intended application. For

TABLE II

FORMAT OF COEFFICIENT DATA FOR CMIP3-DERIVED LTI CLIMATE MODELS IN THE APPENDIX, SAMPLE PERIOD $\Delta = 5$ YEARS

CMIP3 model name	b_4	a_4
	b_3	a_3
	b_2	a_2
	b_1	a_1
	b_0	

application in IAMs, the accuracy is arguably satisfactory, but leaves open the possibility of other (perhaps time-varying) models which better capture the ECS and TCR of the underlying AOGCMs without adversely impacting the feasibility of optimization-based applications such as the estimation of SCC.

Table III shows the results of decomposing each of the 12 low-order climate models $\Delta = 1$ into the implied continuous-time model under ZOH-sampling, i.e. continuous-time impulse response $h(t) = \sum_{i=1}^{4} \theta_i \mathrm{e}^{-t/\tau_i}$. For each model The clear spread of time constant values between τ_1–τ_3 and τ_4 is consistent with a fast–slow decomposition expected in the thermal response of the ocean to radiative forcing, where the upper (mixed) layer warms at rates appreciably faster than the deep ocean.

TABLE III

GAIN FACTOR AND TIME CONSTANTS FOR EACH POLE OF TWELVE LTI APPROXIMATIONS OF CMIP3 CLIMATE MODELS

Model	**Gain factor** ($\times 10^{-3}$)				**Time constant (years)**			
	θ_1	θ_2	θ_3	θ_4	τ_1	τ_2	τ_3	τ_4
CGCM3.1(T47)	91.1	42.1	9.9	1.5	0.78	4.02	18.30	143.73
CNRM-CM3	54.3	30.9	8.1	1.4	0.77	4.28	20.30	160.67
CSIRO-Mk3.0	49.8	31.6	7.0	0.8	0.80	4.04	21.41	210.17
ECHO-G	152.4	32.2	4.5	0.6	1.00	4.94	27.95	162.32
GISS-EH	29.2	20.1	5.2	0.7	0.80	4.21	21.38	181.77
INM-CM3.0	109.9	40.3	7.6	1.0	0.72	3.47	15.55	122.02
IPSL-CM4	56.7	38.4	10.6	1.6	0.80	4.47	23.46	231.45
MIROC3.2(H)	103.3	55.5	17.9	4.2	0.83	4.63	20.81	164.19
MIROC3.2(M)	66.1	44.9	12.5	2.1	0.77	4.40	22.57	207.52
MRI-CGCM2.3.2	86.6	45.8	9.4	1.1	0.65	3.35	16.04	145.58
PCM	34.3	21.5	4.7	0.5	0.68	3.61	18.05	172.58
UKMO-HadCM3	106.7	47.0	10.3	1.5	0.75	3.79	17.23	140.60

IV. CONCLUSIONS

This paper has computed the equilibrium climate sensitivity (ECS) and transient climate response (TCR) for each of the twelve LTI climate models in the model suite, and compared the values so obtained with published values of ECS and TCR for these CMIP3 models. The results of this paper confirm the suitability of simple LTI climate models in IAMs, and quantifies as negligible any loss in accuracy arising from the downsampling of previously obtained models for use in the DICE-2013R IAM. In summary, the results of this paper validate the robustness of conclusions drawn from the application of such models in integrated climate–economy assessments.

REFERENCES

[1] S. J. Phipps, L. D. Rotstayn, H. B. Gordon, J. L. Roberts, A. C. Hirst, and W. F. Budd. The CSIRO Mk3L climate system model version 1.0—Part 1: Description and evaluation. *Geosci. Model Dev.*, 4(2):483–509, 2011.

[2] M. Meinshausen, S. C. B. Raper, and T. M. L. Wigley. Emulating coupled atmosphere-ocean and carbon cycle models with a simpler model, MAGICC6–Part 1: Model description and calibration. *Atmos. Chem. Phys.*, 11(4):1417–1456, February 2011.

[3] W. Nordhaus. Estimates of the social cost of carbon: Concepts and results from the DICE-2013R model and alternative approaches. *J. Assoc. Environ. Resour. Econ.*, 1(1/2):273–312, March 2014.

[4] S. R. Weller, S. Hafeez, and C. M. Kellett. Estimates of the social cost of carbon using climate models derived from the CMIP3 ensemble. In *3rd ASEAN Australian Engineering Congress (AAEC 2015) : Australian Engineering Congress on Innovative Technologies for Sustainable Development and Renewable Energy*, pages 84–89, Singapore, 11–13 March 2015.

[5] S. R. Weller, S. Hafeez, and C. M. Kellett. A receding horizon control approach to estimating the social cost of carbon in the presence of emissions and temperature uncertainty. Accepted to appear, *IEEE Conf. Decis. Control (CDC 2015)*, Osaka, Japan, 15–18 December 2015.

[6] R. S. J. Tol. Estimates of the damage costs of climate change. Part II. Dynamic Estimates. *Environ. Resour. Econ.*, 21:135–160, February 2002.

[7] C. W. Hope. Optimal carbon emissions and the social cost of carbon over time under uncertainty. *The Integrated Assessment J.*, 8(1):107–122, 2008.

[8] United States Government Interagency Working Group on Social Cost of Carbon. Technical Support Document: Technical Update of the Social Cost of Carbon for Regulatory Impact Analysis - Under Executive Order 12866. Technical report, May 2013.

[9] G. H. Roe and M. B. Baker. Why is climate sensitivity so unpredictable? *Science*, 318:629–632, October 2007.

[10] W. D. Nordhaus and P. Sztorc. *DICE 2013R: Introduction and User's Manual*, second edition, 31 October 2013. Available at http://www.econ.yale.edu/∼nordhaus/homepage/.

[11] S. R. Weller, B. P. Schulz, and B. M. Ninness. Identification of linear climate models from the CMIP3 multimodel ensemble. In *Proc. 19th IFAC World Congress, Cape Town, South Africa*, pages 10875–10881, 24–29 August 2014.

[12] D. A. Randall, R. A. Wood, S. Bony, R. Colman, T. Fichefet, et al. Climate models and their evaluation. In *Climate Change 2007: The physical science basis. Contribution of Working Group I to the Fourth Assessment Report of the IPCC (FAR)*, pages 589–662. Cambridge University Press, 2007.

[13] S. Randalls. History of the 2 °C climate target. *Wiley Interdiscip. Rev. Clim. Change*, 1(4):598–605, July/August 2010.

[14] G. A. Meehl, C. Covey, T. Delworth, M. Latif, B. McAvaney, J. F. B. Mitchell, R. J. Stouffer, and K. E. Taylor. The WCRP CMIP3 multimodel dataset. *Bull. Amer. Meteor. Soc.*, 88(9):1383–1394, 2007.

[15] J. D. Annan and J. C. Hargreaves. Understanding the CMIP3 multimodel ensemble. 24(16):4529–4538, August 2011.

[16] U. Cubasch, G. A. Meehl, G. J. Boer, R. J. Stouffer, M. Dix, et al. Projections of future climate change. In *Climate Change 2001: The Scientific Basis: Contribution of Working Group I to the Third Assessment Report of the Intergovernmental Panel*, pages 526–582. Cambridge University Press, Cambridge, United Kingdom and New York, NY, USA., 2001.

[17] IPCC. Summary for Policymakers. In T.F. Stocker et al., editor, *Climate Change 2013: The Physical Science Basis. Contribution of Working Group I to the Fifth Assessment Report of the Intergovernmental Panel on Climate Change*. Cambridge University Press, Cambridge, United Kingdom and New York, NY, USA., 2013.

APPENDIX: CMIP3 LTI MODELS, $\Delta = 5$

Model name	LTI model coefficients	
CGCM3.1(T47)	-0.01515438	0.00035120
	0.14602046	-0.21419255
	-0.15852355	1.23666999
	-0.17335203	-2.01702248
	0.20591106	
CNRM-CM3	-0.00985848	0.00035210
	0.08040311	-0.23739014
	0.00682009	1.30491806
	-0.30793132	-2.06327660
	0.23421046	
CSIRO-Mk3.0	-0.00903861	0.00043412
	0.10880651	-0.22696279
	-0.15725103	1.29101245
	-0.04052582	-2.06115480
	0.09997050	
ECHO-G	-0.04500907	0.00201425
	0.26703749	-0.30456819
	-0.31357874	1.48166344
	-0.06174625	-2.17596763
	0.15544568	
GISS-EH	-0.00547239	0.00044948
	0.03279582	-0.23750128
	0.09595485	1.31243034
	-0.33575092	-2.07145522
	0.21470817	
INM-CM3.0	-0.01315748	0.00016389
	0.14522161	-0.16616689
	-0.21447102	1.09754863
	-0.05978981	-1.92313515
	0.14728929	
IPSL-CM4	-0.01185484	0.00051278
	0.11523484	-0.26137974
	-0.0756595	1.37939386
	-0.24134278	-2.11577250
	0.21654100	
MIROC3.2(H)	-0.02246890	0.00063066
	0.23621936	-0.26233550
	-0.38524770	1.36433436
	0.01657190	-2.09840860
	0.16153780	
MIROC3.2(M)	-0.01300950	0.00039874
	0.16252077	-0.25350924
	-0.25677154	1.35673455
	-0.01761847	-2.10041879
	0.12840392	
MRI-CGCM2.3.2	-0.00896372	0.00007053
	0.13162502	-0.15982261
	-0.20296304	1.09088619
	-0.06227388	-1.92413328
	0.14725787	
PCM	-0.00433128	0.00012215
	0.03649424	-0.18549074
	0.07390895	1.17153542
	-0.31590710	-1.98099426
	0.21236334	
UKMO-HadCM3	-0.01551543	0.00024611
	0.17392451	-0.19432642
	-0.27469837	1.18204755
	-0.02242823	-1.98152548
	0.14381019	